

Design and Prototype of Auto-Track Long-Range Free-Space Optical Communication

Xun Li, Mustafa Mert Bayer, George Nikolaev Guentchev, and Ozdal Boyraz

Electrical Engineering and Computer Science Department, University of California, Irvine, CA 92697, USA

Author e-mail address: xunl12@uci.edu, bayerm@uci.edu, guentchg@uci.edu, and oboyraz@uci.edu

Abstract: We present a free-space optical communication module for the NSF PAWR program with an auto-tracking over $\pm 6.5^\circ$ angle of arrival with $< 1 \mu\text{rad}$ resolution. The module is designed to work for rural area deployment. © 2022 The Author(s)

1. Introduction

In recent years, free-space optical (FSO) communication systems attracted researchers' interest with their low cost and easy-to-deploy features. With the popularization and prosperous market of the Internet, the demand to establish high-speed and low-cost data communication is massively increased. As early as 1962, MIT Lincoln Labs demonstrated an FSO television signal link using a light-emitting GaAs diode, even prior to the invention of reliable lasers, which creatively generate the concept of FSO communications. After 1965, more demonstrations were performed as available lasers came out but the results are always not promising due to the divergence angle and weather turbulence [1]. After the debut of low-loss fiber optics, FSO communication is faded out of the sight since the 1970s [2]. However, for remote areas, the low population and isolated location make traditional fiber optics communication costly and unachievable, which points out the FSO communication systems as an alternative. In 2006, K. Kazaura, et al, experimentally demonstrated a compact beacon system at 980 nm with different levels of tracking precision by using a CCD camera and quadrant detector [3], while another beacon tracking system with a fast steering mirror was discussed in 2011 [4]. It should be considered that, in real practice, the optical power will be influenced by multiple factors, including misalignment and geometric loss [2].

In this work, we design an FSO communication telescope unit that operates at e-band with multiple channels in ITU grid to realize a data transfer with 100Gb/s using an optical collimator (CL) with $35 \mu\text{rad}$ divergence angle. The potential walk-off, the mismatch in the angle of incidence, and the effect of the weather conditions can easily mitigate fiber coupling efficiency. Thus, a multi-level (coarse/fine/ultra-fine) self-alignment system is necessary. This is accomplished by a 980nm beacon light and via two high-resolution ($0.23 \mu\text{rad}$ per micro-step) rotational stepper motors. In the beacon architecture, an additional CL is used to transmit the beacon light with a larger divergence angle (0.8mrad), which reduces the difficulty to locate the beam by generating a 16m diameter spot size on the receiver site. Moreover, the 980nm beacon is modulated with on-off keying (OOK) modulation that has a rate of $< 1\text{Mb/s}$ to realize a supervisory communication channel for handshaking purposes. On the receiver side, the alignment is realized by a metal-oxide-semiconductor (CMOS) camera and a Si avalanche photodiode (APD) combined with different lens assemblies for collection optimization. An auto-track feedback scanning algorithm controls the motorized stages by using the information from the CMOS, APD, and the communication signal levels to secure the communication link.

2. FSO Telescope Design and Required Parameters

The goal of the design is to achieve more than 6km free-space data communication at e-band between nodes to obtain an FSO communication network system fully functioning at least 50% time of the day. The signal branch has a CL with 88mm aperture and $35 \mu\text{rad}$ beam divergence that results in a $\sim 70\text{cm}$ diameter spot size at the receiver unit at 20km, which massively raises the power capacity of the optical branch due to the low geometric loss. The optical backbone of the communication unit is realized via combining 16 dense wavelength-division-multiplexing (DWDM) SFP+ transceivers with $\sim 10\text{Gb/s}$ data rate that can yield a total of $> 100\text{Gb/s}$ data transmission capacity. Edge switches are programmed to enable or disable unused channels and control channel capacity from 10GB/s to 160Gb/s and the power per channel based on the feedback system. The total output of the channels is further amplified by an erbium-doped fiber amplifier (EDFA) with gain flatness of 2dB and gain saturation of 33dBm. The amplified signal is then further transmitted to the output CL through a circulator. On the receiver end, the minimum resolvable power by the transceiver is -23dBm yielding a 50dB margin for losses due to coupling, propagation, weather, etc. Each component of the telescope unit is illustrated in Fig. 1(a).

The beacon system operates at 980nm and the beam divergence of the beacon CL is designed as 0.8mrad to obtain a 16m diameter spot size at the receiver end. The transmitted beam is modulated with a 1Mb/s data rate as a supervisory channel to realize the handshaking protocols. The reception branch has a 100mm^2 Si free-space APD with tunable trans-impedance amplifier (TIA) gain to realize various levels of alignment accuracy. Based on the gain-bandwidth

product, it is possible to tune the bandwidth (BW) of the APD. A 50mm double-convex lens is placed before the APD to improve the collection by considering the detector is not responsive to the potential aberrations. Besides, the large area of the sensor will also improve the angle of view of the beacon. Thus, the APD detector will provide the most coarse alignment during the scanning process.

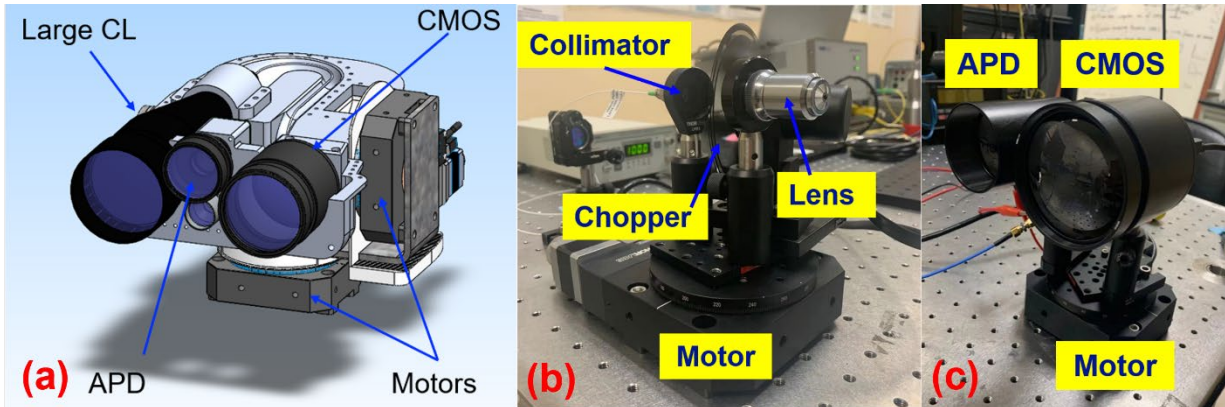


Fig. 1 (a) The main assembly of the telescope consisting of signal, APD, and CMOS units. (b) The transmitter was used in the angle-of-arrival experiments. (c) APD and CMOS on the rotational motor in the experiment.

To realize fine alignment, a 28mm^2 CMOS camera with $3.45\mu\text{m}$ by $3.45\mu\text{m}$ pixel size is integrated with a 75mm aspherical lens that has a 50 mm focal length to focus the spot on the CMOS camera with a minimal spot size by eliminating most of the aberration effect. The spot will move on the CMOS camera from one pixel to the other based on the deviation in the angle of incidence. Reducing the spot size and enlarging the focal length of the lens can enhance the responsivity of the detector in terms of defining the beam walk-off. At 20 km, the focused spot size is simulated using Zemax and found as $1.67\mu\text{m}$ by considering the incident beam as a plane wave. Therefore, the pixel-to-pixel shift can be captured and used to navigate the telescope via the CMOS camera. Moreover, the narrow-band 980nm filters are added to the optical path of both APD and CMOS for isolation of the beacon light by considering the solar spectrum.

Overall, the coarse alignment will be performed with the largest step size until the spot is within the active area of the CMOS camera, while the APD is set to have a high gain and low BW. The APD voltage information provides the boundaries for the CMOS. Then, the spot will be navigated by fine steps, where the step size is no more than the angular resolution of the camera that is about $\sim 30\mu\text{rad}$. After the spot is localized at the CMOS, the ultrafine alignment to maximize the fiber coupling efficiency via the signal CL is realized by utilizing the power readings through the transceivers as the last feedback mechanism along with the APD and CMOS, where the maximum resolution of the motors is used. The motor resolution is determined by the gear ratio and the steps per revolution provided by the motor controller. In the current design, the gear ratio is 66:1, and micro-steps per revolution is 409,600 that results in a step resolution of $0.23\mu\text{rad}$ to realize the fiber coupling.

4. Results

To demonstrate the capability of the optical system, we performed experiments and simulations. The goal of the first experiment is to verify the angle of arrival of the APD. As shown in Fig. 1(b-c) on the rotational stages, the 980nm laser is connected with a collimator. Due to the distance limitations in the lab, we put an objective lens after the collimator to diverge the beam with a full divergence angle of 58° to realize a plane wave-like spot on the receiver. An optical chopper is also used to mimic the behavior of modulation. On the receiver side which is 1.2 m away, the APD and CMOS are attached to the motorized stage along with their collection optics. By rotating the stage, it is found out that the reception angle is around $\pm 6.5^\circ$. In total, a 13° range angle is advantageous to not only the initial installation but also the tracking of the beam. The modulation of the beacon light is also realized in different frequencies between 1kHz-1MHz with both chopper and direct modulation of the laser.

The minimum angular resolution is a crucial factor to evaluate the FSO communication system. However, experimenting with long distances is not possible in the early stages of design. Therefore, we perform pixel-to-pixel CMOS simulations on Zemax assuming the CMOS camera has sufficient sensitivity. In the first simulation, we set the incident beam as a perfect planar Gaussian beam at 980nm. The schematic of the simulation to acquire the minimum spot size with the planar wave is demonstrated in Fig. 2(a) and the heatmap of the resultant spot diagram is illustrated in Fig. 2(b). With the focalization of the beam due to the 75mm aspheric lens ($f=50\text{mm}$), the simulation indicates the minimum spot diameter at the focal point as $1.67\mu\text{m}$, which is smaller than the pixel size of $3.5\mu\text{m}$.

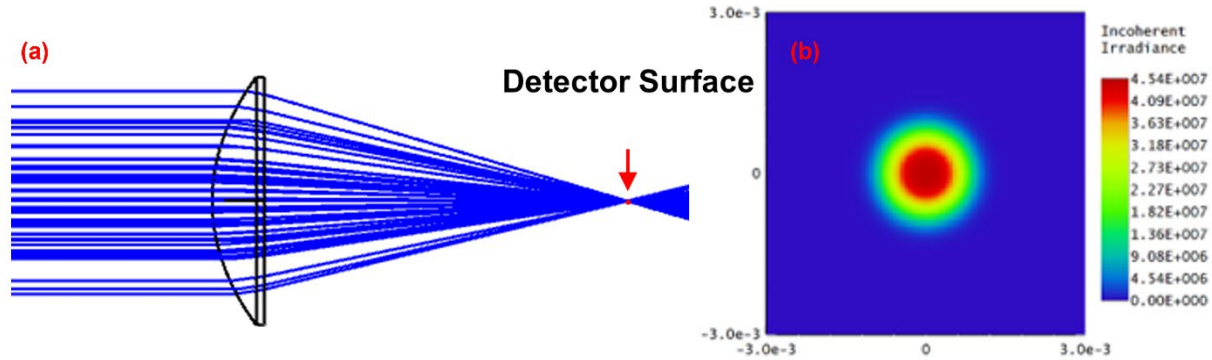


Fig. 2 (a) Schematic of the simulation of the spot size with a perfect planar Gaussian beam. (b) The resultant heatmap of the spot on the CMOS and units is in mm.

In the second simulation, we introduced the beacon CL into the system and extended the simulation distance L to 20km as depicted in Fig. 3. Tilting the beam by θ will result in the movement of the spot on the CMOS active area. The displacement of the spot can be distinguished only if the movement distance is larger than the length of the pixel of the camera. To realize the motion of the spot, two pixel-areas are created in Zemax as shown in Fig. 4, representing pixel 0 at the normal line and the neighboring pixel 1, respectively. The result shows that to obtain a pixel-center to pixel-center shift, the minimum angle θ is $30.2\mu\text{rad}$, which is in an acceptable range compared with the minimum step size of the stepper motor ($0.23\mu\text{rad}$).

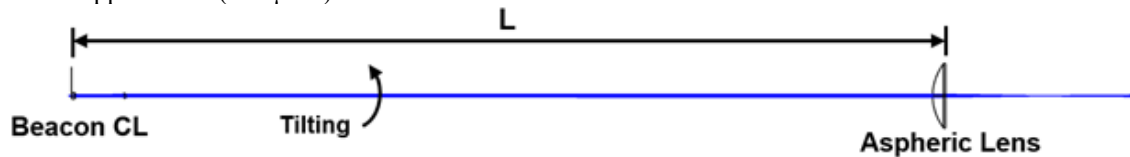


Fig. 3 Schematic of the simulation using Zemax to realize the minimum resolvable angle.

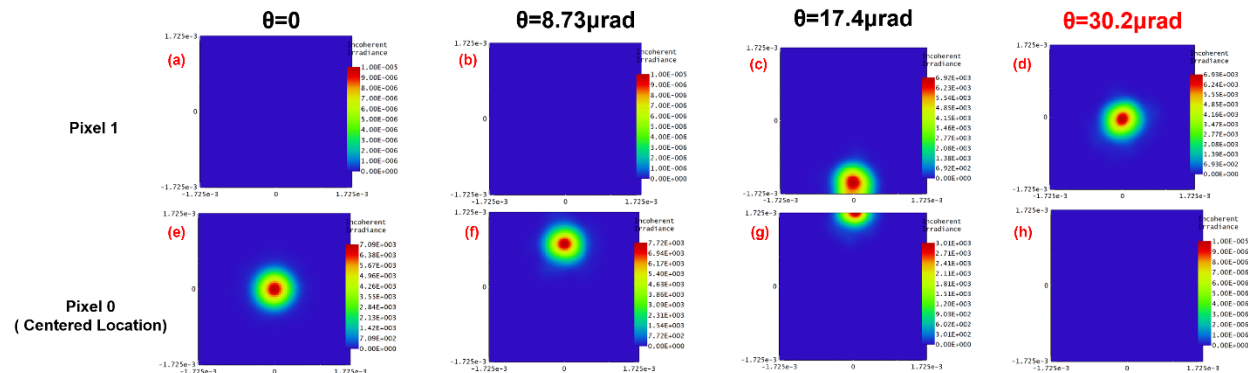


Fig. 4 Pixel-to-pixel movement of the spot due to angular deviation. (a-d) Active area of CMOS at pixel 1. (e-h) Active area of CMOS at pixel 0.

5. Conclusion

We present the design of a prototype of a multi-level auto-track FSO communication system, including a CMOS camera and a Si-APD detector. The experimental and simulation results are presented, indicating a wide field of angle and high angular resolution of the beacon system along with the high-resolution gimbal to realize the FSO communication.

6. Acknowledgment

This work was supported by the NSF under grant number PAWR-5582469.

7. References

- [1] F. E. Goodwin, "A review of operational laser communication systems," *Proceedings of the IEEE* **58**, 1746–1752 (1970).
- [2] M. A. Khalighi and M. Uysal, "Survey on Free Space Optical Communication: A Communication Theory Perspective," *IEEE Communications Surveys Tutorials* **16**, 2231–2258 (2014).
- [3] K. Kazaura, K. Omae, T. Suzuki, M. Matsumoto, E. Mutafungwa, K. Asatani, T. Murakami, K. Takahashi, H. Matsumoto, K. Wakamori, and Y. Arimoto, "Experimental demonstration of next-generation FSO communication system," in *Broadband Access Communication Technologies* (SPIE, 2006), Vol. 6390, pp. 130–141.
- [4] Y. Arimoto, "Multi-Gigabit Free-Space Laser Communications Using Compact Optical Terminal with Bidirectional Beacon Tracking," in *2011 IEEE International Conference on Communications (ICC)* (2011), pp. 1–5.